BIOINFORMATION
Discovery at the interface of physical and biological sciences

open access www.bioinformation.net Hypothesis

Volume 8(12)

Qualitative and Quantitative analysis of 3D predicted arachidonate 15-lipoxygenase-B (15-LOX-2) from *Homo sapiens*

Neha Arora[1], Vinay Kumar Singh[2], Kavita Shah[3] & Shashi Pandey-Rai[1]*

[1]Laboratory of Morphogenesis, CAS in Botany, Faculty of Science, Banaras Hindu University, Varanasi-221005; [2]Bioinformatics Center, School of Biotechnology, Banaras Hindu University, Varanasi; [3]IESD, BHU, Varanasi; Shashi Pandey-Rai shashi.bhubotany@gmail.com; *Corresponding author

Received June 05, 2012; Accepted June 09, 2012; Published June 28, 2012

Abstract:
15-Lipoxygenase-2 protein has been reported to play an important role in normal development of prostate, lung, skin, and cornea tissues. It behaves as a suppressor of prostate cancer development by restricting cell cycle progression and implicating a possible protective role against tumor formation. On the basis of the above report, we selected 15-LOX-2 protein to study the structural classification and functional relationship with associated protein network at computational level. Sequence alignment and protein functional study shows that it contains a highly conserved LOX motif. PLAT domain with PF01477 and LH2 domain with PF00305 were successfully observed. Arachidonate 5-lipoxygenase (PDB ID: 3O8Y) was selected as a template with 42% identity. 3D structure was successfully predicted and verified. Qualitative analysis suggests that the predicted model was reliable and stable with best quality. Quantitative study shows that the model contained expected volume and area with best resolution. Predicted and best evaluated model has been successfully deposited to PMDB database with PMDB ID **PM0078035**. Active site identification revealed GLU[369], ALA[370], LEU[371], THR[372], HIS[373], LEU[374], HIS[376], SER[377], HIS[378], THR[385], LEU[389], HIS[394], PHE[399], LYS[400], LEU[401], ILE[403] and PRO[404] residues may play a major role during protein-protein, protein-drug and protein-cofactor interactions. STRING database result indicated that IL (4), GPX (2 and 4), PPARG, PTGS (1 and 2), CYP (2J2, 2C8, 4A11 and 2B6), PLA (2G2A, 2G4A, 2G1B and 2G6) and A LOX (5, 15, 12 and 12B) members from their respective gene families have network based functional association with 15-LOX-2.

Keywords: Qualitative, Quantitative, 3D structure, Ramachandran plot, LOX motif

Background:
Lipoxygenases (LOX) are non-heme, iron-containing lipid-peroxidizing enzymes that use molecular oxygen for the dioxygenation of arachidonic acid. They catalyze the formation of hydroperoxides as the first step in the biosynthesis of several inflammatory mediators like leukotrienes and lipoxins **[1-3]**. The protein consists of a small N-terminal PLAT domain and a major C-terminal catalytic domain containing the active site. The iron atom in LOX is bound by four ligands among which three are histidine residues. Six histidines are conserved in all lipoxygenase sequences, five of them are clustered in a stretch of 40 amino acids. The structure of soybean lipoxygenase-1, determined by X-ray diffraction methods, reveals that 839 amino acids in the protein are organized in two domains viz. beta-sheet N-terminal domain and helical C-terminal domain **[1]**. LOX are classified according to their positional specificity of the dioxygenation of their most common substrates linoleate (C-18) in plants, and arachidonic acid (C-20) in mammals **[2]**. In mammals, LOX have been classified as 5-, 8-, 12-, and 15-LOX. These LOX oxygenate at carbon 5, 8, 12 or 15 of arachidonic acid, forming 5S-, 8S-, 12S-, or 15S-hydroperoxyeicosatetraenoic acid (5-, 8-, 12-, or 15-HPETE) respectively. HPETEs are further

reduced by glutathione peroxidase to 5-, 8-, 12-, 15-HETE, which are the hydroxy forms. 15-LOX exists as two isozymes, 15-LOX-1 and 15-LOX-2. The substrate for 15-LOX-1 and 15-LOX-2 are linoleic acid and arachidonic acid, respectively **[4, 5]**. 15-LOX-2 is recently cloned human lipoxygenase that shows tissue-restricted expression in prostate, lung, skin, and cornea. The protein level and enzymatic activity of 15-LOX-2 have been shown to be down-regulated in prostate cancers compared with normal and benign prostate tissues **[6]**. Since, 15-LOX-2 structure is not available in any protein structure database so far to understand the functional behavior of this protein, so an *in-silico* study, mainly comparative homology modeling, of the target sequence 15-LOX-2 can be helpful to investigate sequential-structural-functional relationship. 3D structure of 15-LOX-2 was predicted based on available homologous template structure in Protein structure Data Bank resources. Template selection was performed using Protein Data Bank (PDB) advanced BLAST **[7]**. Retrieved template structure was used for comparative homology modeling of 15-LOX-2 protein.

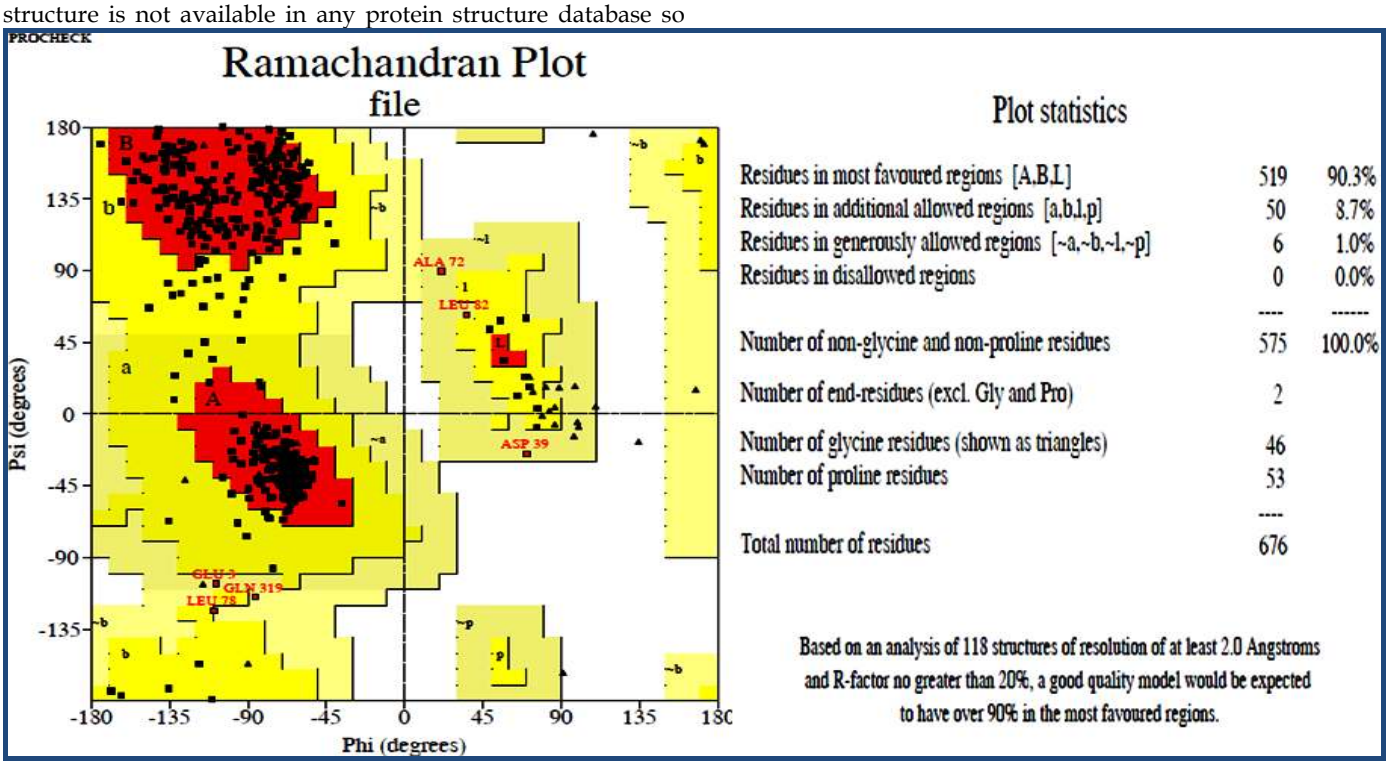

Figure 1: Ramachandran plot graphical representation with plot statistics

Methodology:

Retrieval of the target protein sequence

The protein sequence of 15-lipoxygenase B isoform d (15-LOX-2) from *Homo sapiens* was obtained from the protein sequence database of NCBI (Accession No: NP_001132.2) **[8]**. Since three dimensional structures of 15-LOX-2 for *Homo sapiens* is not available in Protein structure database (PDB) **[9]**, hence an attempt has been made in the present study to determine the 3D structure of 15-LOX-2 to decipher the functional role of structural motif and secondary elements. ProtParam server **[10]** was used for computation of various physical and chemical parameters for selected protein.

Template Identification

The NCBI BLAST was used to identify the template for modeling the three dimensional structure of 15-LOX-2 from *Homo sapiens*. The result of NCBI BLAST against the PDB database was used for selection of a suitable template for 3D modeling of the target protein.

Sequence alignment

15-LOX-2 amino acid sequence was used for alignment with template protein using BLAST (bl2seq) **[11]**. Default parameters were applied and the aligned sequences were inspected and adjusted manually to minimize the number of gaps and insertions.

Homology modeling and Structure refinement

The three dimensional structure of 15-LOX-2 has been predicted using DS MODELLER. A rough 3D model was constructed based on sequence alignment between 15-LOX-2 of *Homo sapiens* and the template proteins using Discovery studio 3.1 **[12]** with selected parameters. Loop refinement and structural simulation were done using LOOPER and CHARMm forcefield, respectively. Finally, predicted 3D model was subjected to a series of tests for testing its internal consistency and reliability. The Quality of the model was checked with verify3D **[13]**, Profile 3D **[14]** and Errat **[15]** and the stereochemical properties based on backbone conformation were evaluated by inspection of Psi/Phi/Chi/Omega angle using Ramachandran plot of PDBSum database **[15, 16]**. Quantitative analysis was done using accessible surface area prediction using Volume Area Dihedral Angle Reporter (VADAR) **[17, 18]**. Standard bond lengths and bond angles of the model were determined using WHAT IF **[15, 19 & 20]**. ResProx (Resolution-by-proxy) **[21]** was also used for quality and quantity measurment using Standard deviation of $\chi 1$ pooled, Ramachandran outside of most favored, Deviation of Θ angles, Bump score, Mean H-bond energy, $\chi 1$ score, Radius gyration score, Percentage of generously allowed Ω angles, Percentage of packing defects, Percentage of 95% buried residues, Percentage of bad bond length, Percentage of bad bond angles and Ramachandran plot outliers.

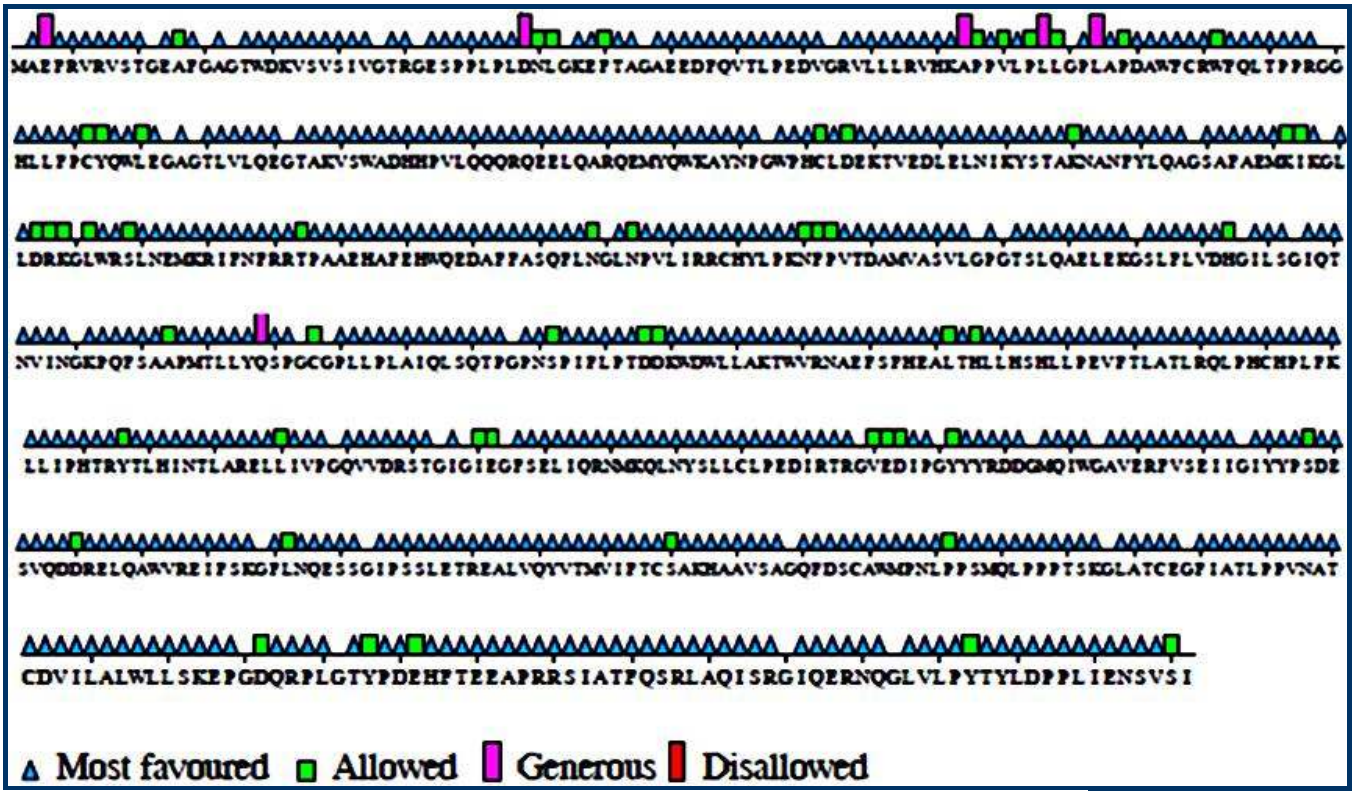

Figure 2: 1D representation of residues found in most favoured, allowed and generous allowed region

Structure Submission

Successfully modeled, verified and the most reliable structure of 15-LOX-2 was used for deposition in PMDB (Protein Model Database) database **[22]**.

Active Site Prediction

After complete modeling, simulation and refinement of the structure of 15-LOX-2, it was used for prediction of the possible binding sites using Q-SiteFinder **[23]**. Ten binding sites were predicted for the target protein. These binding sites were further compared to the active sites of the template.

Prediction of Protein- Protein interaction network

Protein–Protein functional association network was predicted using STRING database version 9.0 **[24]**.

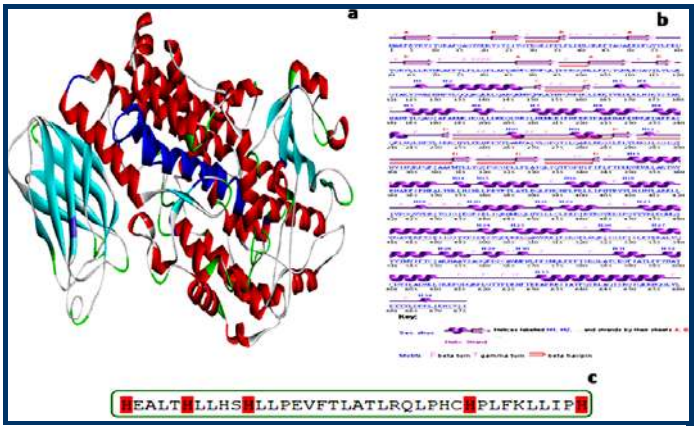

Figure 3: (a) Modeled structure of Arachidonate 15-Lipoxygenase-B isoform d where α-helices have been represented by red color, ß-sheets by cyan, loops in green and the blue color indicates the LOX motif; **(b)** Figure depicting the sheets, beta hairpins, beta bulges, strands, helices, helix- helix interacs, beta turns and gamma turns present in the model; **(c)** 1D sequence of LOX motif where red color represents conserved histidine residues

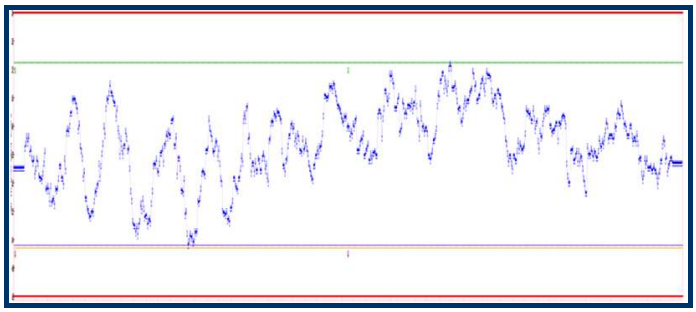

Figure 4: Showing VERIFY 3D interpretation

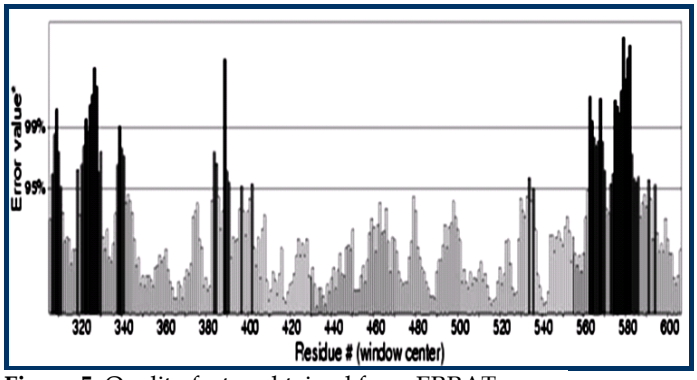

Figure 5: Quality factor obtained from ERRAT server

Results:

The selected protein 15-lipoxygenase B (NP_001132.2) has 676 amino acids in length with molecular weight of ~75 kDa. It is 12.4% highly Leucine rich with theoretical pI 5.73. On the basis of sequence similarity analysis, Arachidonate 15-Lipoxygenase-B isoform d showed 62% sequence similarity and 42% identity with template structure (PDB ID 3O8Y). Since the template showed a good level of sequence identity it was used to obtain high quality alignment for structure prediction using homology modeling. A PDB ID 3O8Y crystal structure of stable-5-Lipoxygenase from Human was specifically selected on the basis of BLAST result and was utilized as a template for structure modeling of 15-LOX-2. Structural model was built based on the atomic coordinates of 3O8Y using modeling and simulations program of DS MODELER **[25]**. The loop refined model, which was selected with minimum CHARMm energy 40839.47232 kcal/mol based on conjugant gradient minimization, was considered for quality and quantity evaluation.

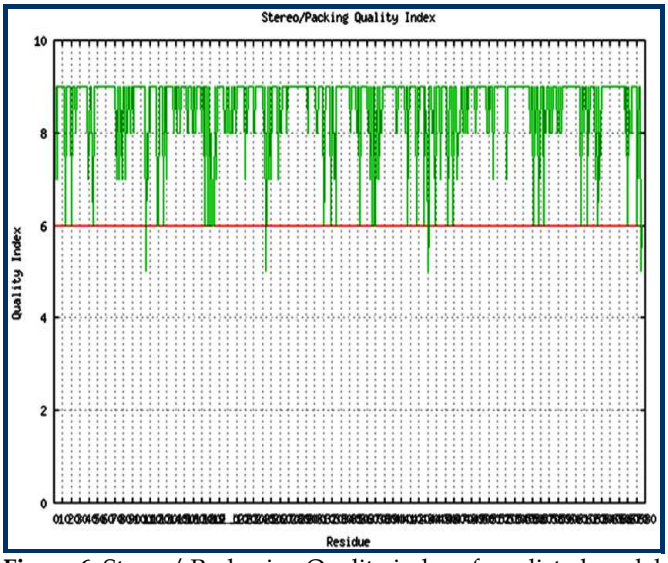

Figure 6: Stereo/ Packaging Quality index of predicted model

3D predicted model was analyzed using energy minimization, refinement and simulation programs of Discovery studio 3.1. PROCHECK of PDBSum server was employed for the evaluation of stereochemical quality of predicted model. Ramachandran plot analysis showed 90.3 % of amino acid residues within the most favoured and 9.7% residues in additional and generously allowed regions, whereas no residue was found in disallowed region **(Figures 1, 2)**. The structural model of 15-LOX-2 is shown in **(Figure 3a).** The comparable Ramachandran plot characteristic and G-factor score confirmed the good quality of the predicted model. Based on main-chain and side-chain parameters study, we found that the confirmation of the predicted model was very much favourable, stable and reliable. The 15-LOX-2 model consists of two domains: N-terminal contains Polycystin-1, Lipoxygenase, Alpha-Toxin (PLAT; 4-119) domain, totally arranged with beta sheets and C-terminal has Lipoxygenase homology (LH2; 197-668) domain, with α-β fold type mainly contains alpha helices. Structural classification of the predicted model revealed that PLAT domain contains only beta sandwich with CATH ID 1.20.245.10 and LH2 domain has mainly alpha fold of up-down bundle type with CATH ID 2.60.60.20. In this predicted 3D model 4 sheets, 7 beta hairpins, 5 beta bulges, 15 strands, 34 helices, 52 helix- helix interacs, 53 beta turns and 7 gamma turns were analyzed using PDBSum. The LOX-motif contains only helical arrangement **(Figures 3b, c)**.

Qualitative and quantitative study of predicted model

VERIFY 3D details lie between 0.01 – 0.74 representing the best verified and reliable model **(Figure 4)**. Overall quality factor was calculated with ERRAT server **[26]** and the modeled structure was found to have 74.738 % quality factor **(Figure 5)**. VADAR that included accessible surface area, excluded volume, backbone and side chain dihedral angles, secondary structure, hydrogen bonding partners, hydrogen bond energies, steric quality, solvation free energy as well as local and overall fold quality yielded good results **(Figure 6)**. Using atomic radii from Shrake method, we observed 41% residues were involved in the formation of helices, 18% in beta sheets, 40% in coils and 19% residues formed turns. Observed mean hbond distance and energy value were closely similar with expected values in hydrogen bond statistics. The obtained expected residues with hbond were 75% and we observed 74% for the predicted model. Dihedral angle statistics also represented approximately similar score with that of the expected values **Tables 1a, b (see supplementary materiel)**. Normality test of the predicted structure checked using WHATIF was found to have fine packing quality with Z-score of 0.06. Resprox result infer that the resolution of the predicted model was 2.695 Å. Deviation of Θ angles, Bump score, χ1 score and Radius gyration Z- score indicate better quality of the model **Table 2 (see supplementary materiel))**. It was found that the overall quality and quantity on the basis of secondary elements of the predicted model was good and reliable. Predicted and completely analyzed model of 15-LOX-2 was successfully deposited in PMDB (Protein Model Database) **[27]** database with PMDBID **PM0078035**. The RMSD (Root Mean Square Deviation) between predicted model and template is 0.34 Å with Z-score 1.9122E+02 using AuStrAliS server **[28] (Figure 7)**.

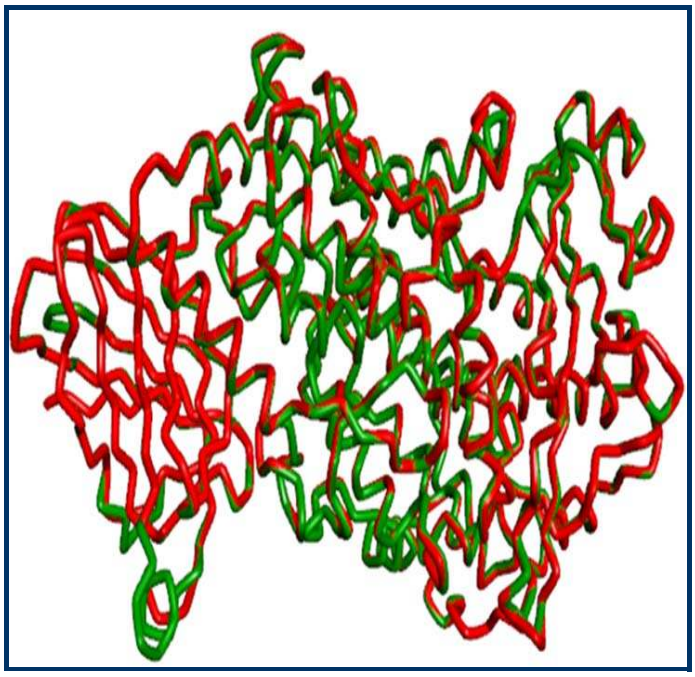

Figure 7: Superposed structure of Target (Green) and Template (Red**)**

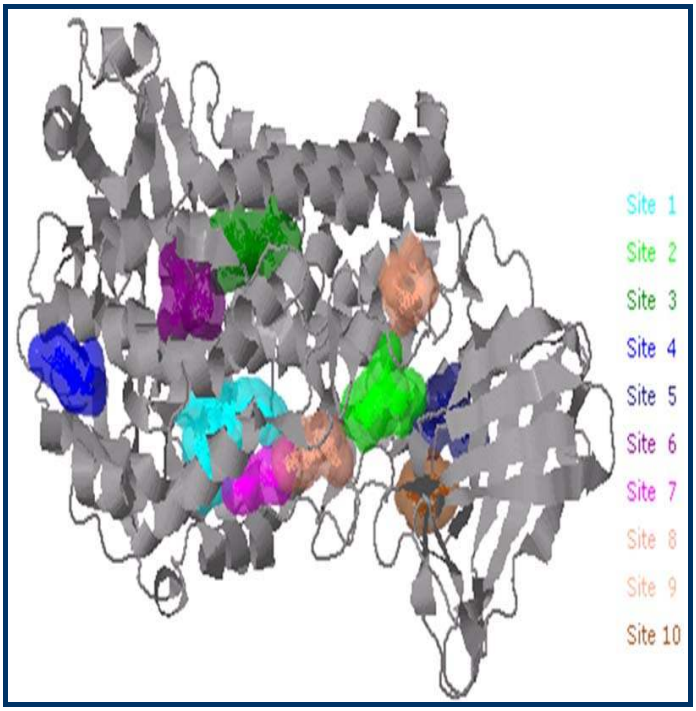

Figure 8: Figure showing the 10 possible active sites (in different colors) in the predicted 3D model

Active site analysis

Active site identification of 3D predicted model 15-LOX-2 with PMDBID **PM0078035** from *Homo sapiens* was done using Q-siteFinder. 10 possible active binding sites were localized in the predicted model **(Figure 8, 9)**. All 10 predicted site volumes with their active binding residues are reported in **Table 3 (see supplementary materiel)**.

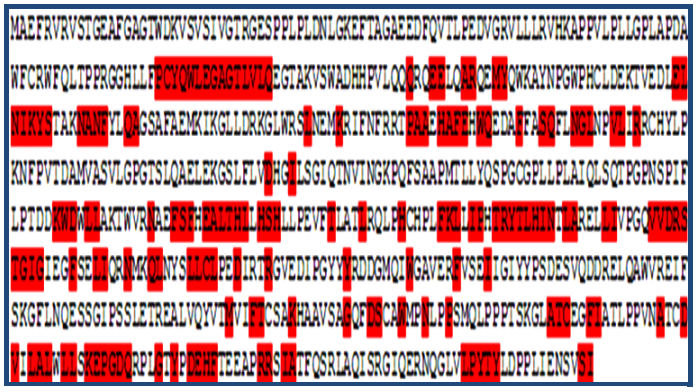

Figure 9: 1D protein sequence representation of active sites in red color

Protein–Protein functional association network

Protein–protein interactions occur when two or more proteins interact together to carry out their biological functions. These interactions are important for every biological process in a living cell. Protein-protein interaction helps in understanding of systems biology at structural domain and motif level and provides the basic knowledge for the application of therapeutic drug targets. In this *in-silico* investigation, 15-LOX-2 (NP_001132.2) protein was used to find out the association network with similar function of proteins. It was found that 15-LOX-2 has 19 major association networks with 7 types of protein families, including LOX gene family. IL (4), GPX (2 and 4), PPARG, PTGS (1 and 2), CYP (2J2, 2C8, 4A11 and 2B6), PLA (2G2A, 2G4A, 2G1B and 2G6) and A LOX (5, 15, 12 and 12B) gene families were found to have maximum STRING score 0.900 with highest confidence level **(Figures 10 a, b) [29]**.

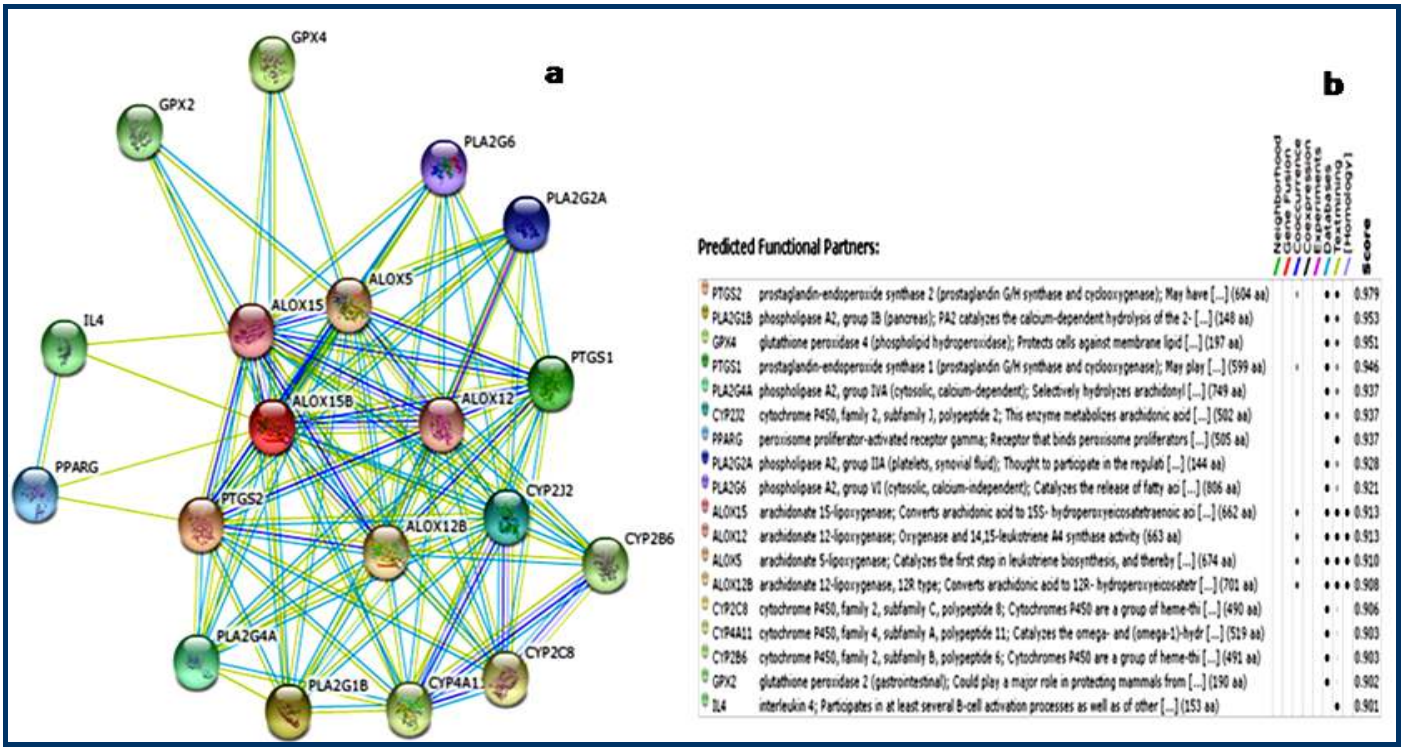

Figure 10: **(a)** Protein-Protein interaction network with highest confidence with no more than 50 interactions; **(b)** Tabular representation of the interacting partners of 15-LOX-2 protein.

Discussion:
Protein structural modeling and simulations of 15-LOX-2 protein was successfully completed. The Ramachandran plot statistics resulted that 100% residues were found in allowed regions whereas not even a single residue was present in disallowed or in outlier regions. Qualitative and quantitative analysis of the predicted model represented the best quality model which was reliable and stable. In the predicted model, hydrogen bonds (mean hbond distance, mean hbond energy and residues with hbonds) were arranged with good confirmations. Resolution of the predicted model was 2.695 Å. After complete qualitative and quantitative analysis, predicted model has been successfully deposited in PMDB Database with PMDBID **PM0078035**. In LOX motif GLU^{369}, ALA^{370}, LEU^{371}, THR^{372}, HIS^{373}, LEU^{374}, HIS^{376}, SER^{377}, HIS^{378}, THR^{385}, LEU^{389}, HIS^{394}, PHE^{399}, LYS^{400}, LEU^{401}, ILE^{403} and PRO^{404} residues were found to be prominent active binding sites for protein-protein, protein-drug and protein-cofactor interactions.

The STRING based protein–protein interactions elucidated that 7 different protein families were associated in network with 15-LOX-2. Amongst which Interleukin 4 (IL-4) is known to participate in several B-cell activation. It is also a co-stimulator of DNA-synthesis which induces the expression of class II MHC molecules on resting B-cells. Whereas, Glutathione peroxidase (GPX) protects cells against membrane lipid peroxidation and cell death. It is required for normal sperm development, male fertility and is essential for embryonic development. Another interacting protein Peroxisome proliferator-activated receptor gamma (PPARG) is a receptor that binds peroxisome proliferators such as hypolipidemic drugs and fatty acids, thus controlling the peroxisomal beta-oxidation pathway of fatty acids. Prostaglandin-endoperoxide synthase 1 (PTGS) plays an important role in regulating/promoting cell proliferation in some normal and neoplastically transformed cells, whereas PTGS2 functions as a mediator of inflammation and/or plays a role in prostanoid signaling in activity-dependent plasticity. Cytochrome (CYP) P450, family2, subfamilyJ, polypeptide2 is an enzyme that metabolizes arachidonic acid, predominantly via a NADPH-dependent olefin epoxidation, to all four regioisomeric cis-epoxyeicosatrienoic acids. Phospholipase A2, group IIA (platelets, synovial fluid), belonging to PLA family of proteins, participates in the regulation of phospholipid metabolism in biomembranes including eicosanoid biosynthesis. PLA2, G-IVA (cytosolic, calcium-dependent) selectively hydrolyzes arachidonyl phospholipids in the sn-2 position releasing arachidonic acid. PLA2, G-IB (pancreas) catalyzes the calcium-dependent hydrolysis of the 2- acyl groups in 3-sn-phosphoglycerides and PLA2, G-VI (cytosolic, calcium-independent) catalyzes the release of fatty acids from phospholipids. Arachidonate 15-lipoxygenase (A LOX) converts arachidonic acid to 15S- hydroperoxy-eicosatetraenoic acid and acts on C-12 of arachidonate as well as on linoleic acid.

Acknowledgement:
The authors are grateful to the Department of Biotechnology for Financial support provided in the form of a project to Dr. Shashi Pandey. They also wish to acknowledge the facility provided by Department of Biotechnology funded Sub-Distributed Information Centre, Centre for Bioinformatics, School of Biotechnology, Banaras Hindu University, and Varanasi, India.

References:
[1] Prigge ST *et al. Biochimie.* 1997 **79 :** 629 [PMID: 9479444]
[2] Andreou A & Feussner I, *Phytochemistry.* 2009 **70 :**1504 [PMID: 19767040]
[3] Nelson MJ & Seitz SP, *Curr Opin Struct Biol.* 1994 **4:** 878 [PMID: 7712291]
[4] Schewe T *et al. Prostaglandins Leukot Med.* 1986 **23** 155 [PMID: 3094029]
[5] Kühn H & Borngraber S, *Adv Exp Med Biol.* 1999 **447:** 5 [PMID: 10086179]
[6] Tang S *et al. J Biol Chem.* 2002 **277:** 16189 [PMID: 11839751]
[7] http://www.rcsb.org/pdb/search/advSearch.do
[8] http://www.ncbi.nlm.nih.gov/entrez/
[9] http://www.rcsb.org/
[10] http://web.expasy.org/protparam/
[11] http://blast.ncbi.nlm.nih.gov/Blast.cgi
[12] Lu SH *et al. J Biomed Sci.* 2011 **18:** 8 [PMID: 21251245]
[13] Eisenberg D *et al. Methods Enzymol.* 1997 **277:** 396 [PMID: 9379925]
[14] Suyama M *et al. J Mol Evol.* 1997 **1:** S163 [PMID: 9071025]
[15] Gundampati RK *et al. J Mol Model.* 2012 **18:** 653 [PMID: 21562828]
[16] http://www.ebi.ac.uk/pdbsum/
[17] http://vadar.wishartlab.com/
[18] Willard L *et al. Nucleic Acids Res.* 2003 **31:** 3316 [PMCID: PMC168972]
[19] http://swift.cmbi.ru.nl/whatif/
[20] Vriend G, *J Mol Graph.* 1990 **8:** 52 [PMID: 2268628]
[21] http://www.resprox.ca/
[22] http://mi.caspur.it/PMDB/
[23] http://bmbpcu36.leeds.ac.uk/qsitefinder/
[24] http://string-db.org/)
[25] Unissa AN *et al. Bioinformation.* 2009 **4**: 24 [PMCID: PMC2770367]
[26] http://nihserver.mbi.ucla.edu/ERRATv2/
[27] http://mi.caspur.it/PMDB/
[28] http://eds.bmc.uu.se/eds/australis.php
[29] Szklarczyk D *et al. Nucleic Acids Research.* 2011 **39:** D561 [PMID: 21045058]

Edited by P Kangueane
Citation: Arora *et al.* Bioinformation 8(12): 555-561 (2012)

BIOINFORMATION

open access

Supplementary material:

Table 1(a): VADAR statistics report. Secondary elements details with hbond statistics*

VADAR STATS	Using atomic radii from Shrake		Hydrogen Bonds (hbonds)		
Statistic	**Observed**	**Expected**	**Statistic**	**Observed**	**Expected**
# Helix	282 (41%)	-	Mean hbond distance	2.2 sd=0.3	2.2 sd= 0.4
# Beta	123 (18%)	-	Mean hbond energy	-1.6 sd= 0.9	-2.0 sd= 0.8
# Coil	271 (40%)	-	# res with hbonds	501 (74%)	507 (75%)
# Turn	132 (19%)	-			

*The expected values represent those numbers which would be expected for highly Xray and NMR structures

Table 1(b): Dihedral angles observation based on phi, psi, chi and omega calculations**

Statistic	Observed	Expected
Mean Helix Phi	-66.2 sd= 6.7	-65.3 sd=11.9
Mean Helix Psi	-38.2 sd= 20.5	-39.4 sd= 25.5
# res with Gauche + Chi	264 (50%)	290 (55%)
# res with Gauche - Chi	66 (12%)	105 (20%)
# res with Trans Chi	198 (37%)	132 (25%)
Mean Chi Gauche+	-66.1 sd= 6.7	-66.7 sd=15.0
Mean Chi Gauche-	63.0 sd= 6.7	64.1 sd= 15.7
Mean Chi Trans	173.6 sd= 5.8	168.6 sd= 16.8
Std. dev of chi pooled	6.40	15.70
Mean Omega (|omega| > 90)	-178.2 sd= 3.9	180.0 sd=5.8
# res with |omega| < 90	0 (0%)	-

**Expected values obtained from Morris AL, MacArthur MW, hutchinson EG and Thornton JM. Proteins. 1992 Apr; 12 (4): 345-364

Table 2: Quantitative results obtained from Resprox server

Score Name	Quality	Z-score	Description	Program
Standard deviation of χ1 pooled	Good	-0.79	Standard deviation of the χ1 angles among all 3 (gauche-, gauche+, and trans) configurations.	Vadar
Ramachandran outside of most favored	Good	1.06	Percentage of residues outside of the most favored regions of the Ramachandran plot.	GeNMR
Deviation of Θ angles	Good	0.67	Standard deviation of angle between the C-O bond vector of the H-bond acceptor and the O-H(N) bond vector.	PROSESS
Bump score	Good	1.32	The bump score is calculated from the total number of non-bonded atom contacts below 1.3 Å, divided by the total number of non-bonded contacts in the protein.	GeNMR
Mean H-bond energy	Good	0.65	The average hydrogen bond energy is calculated using the H-bond energy function used in DSSP program.	Vadar
χ1 score	Good	1.83	Scaled difference between the standard deviation of the observed χ1 angles and the expected one obtained from high quality protein structures.	PROSESS
Radius gyration score	Good	1.88	Scaled difference between the expected radius of gyration and the observed one. The expected radius of gyration is determined using: Rg = 0.395*N**0.6 + 7.257.	GeNMR
Percentage of packing defects	Good	1.21	This is the percentage of residues with fractional residue volumes greater than 1.20 or less than 0.80. Packing defects indicate the presence of cavities or compressions that are not natural.	Vadar
Percentage of packing defects	Good	1.21	This is the percentage of residues with fractional residue volumes greater than 1.20 or less than 0.80. Packing defects indicate the presence of cavities or compressions that are not natural.	Vadar
Percentage of bad bond length	Good	-0.33	This parameter is calculated as the number of bond angles (divided by the total number of bond angles in the polypeptde) that exceed, by more than 5 standard deviations, the typical bond angles seen in high resolution, high quality structures.	MolProbity

Table 3: Predicted 10 active site residues with their Site Volume in Cubic Angstroms

Site No.	Site Volume (Cubic Angstroms)	Active site residues
Site 1	603	PHE^{184},ASN^{362},PHE^{365},SER^{366},PHE^{367},GLU^{369},ALA^{370},HIS^{373},LEU^{374},HIS^{378},ILE^{412},ASN^{413}, ALA^{416}, LEU^{420},ILE^{421},VAL^{426},VAL^{427},ASP^{428},ARG^{429},SER^{430},THR^{431},GLY^{432},ILE^{433},GLY^{434},PHE^{438},LEU^{441}, ILE^{442},PRO^{572},ALA^{599},ASP^{602}, VAL^{603}, LEU^{605}, ALA ^{606}, LEU^{607},LEU^{610},ILE^{676}
Site 2	472	CYS^{106},TYR^{107},GLN^{108},ARG^{145},TYR^{149},ASN^{173},ILE^{174},LYS^{175},THR^{385},LEU^{389},HIS^{394},PHE^{399},ILE^{403}, PRO^{404},THR^{406},ARG^{407},TYR^{408},THR^{409},LEU^{410},HIS^{411}, ASP^{625},HIS^{627}
Site 3	441	VAL^{249},LEU^{250},ARG^{252},ASP^{291},ILE^{294},PHE^{367},LEU^{371},THR^{372},HIS^{376},SER^{377},ASN^{445},GLN^{448},LEU^{449}, LEU^{453},LEU^{454},CYS^{455},LEU^{456},ASP^{459},ARG^{463},TYR^{473}, TRP^{481}, MET^{544}, PHE^{547}, THR^{548}, LYS^{552}
Site 4	338	LEU^{210},LYS^{214},PHE^{229},GLU^{230},TRP^{232},GLN^{233},LYS^{350},TRP^{351},ASP^{352},LEU^{354},LEU^{355},TRP^{566},ALA^{585}, THR^{586},CYS^{587},PHE^{590},ILE^{591}
Site 5	321	PRO^{105},CYS^{106},GLN^{108},THR^{115},LEU^{116},VAL^{117},LEU^{118},GLN^{119},GLN^{137},GLU^{140},GLU^{141},ALA^{144},ARG^{145},MET^{148},TYR^{149},ASN^{173},HIS^{394}
Site 6	287	PRO^{223},ALA^{224},ALA^{225},HIS^{227},ALA^{228},PHE^{237},SER^{240},GLN^{241},ASN^{244},GLY^{245},LEU^{246},GLY^{559},ASP^{562}, SER^{563},ASN^{569},LEU^{660},PRO^{661},TYR^{662},THR^{663},TYR^{664}
Site 7	229	TYR^{176},ALA^{182},ASN^{183},PHE^{184},GLN^{187},ALA^{188},ILE^{412},LEU^{415},LEU^{420},VAL^{426},LEU^{605},ALA^{606},LEU^{609}, LEU^{610},SER^{675},ILE^{676}
Site 8	229	TYR^{176},SER^{177},ASN^{181},ALA^{182},GLN^{187},TYR^{408},LEU^{609},LYS^{612},GLU^{613},PRO^{614},GLY^{615},ASP^{616},GLN^{617}, SER^{675},ILE^{676}
Site 9	219	LYS^{400},LEU^{401},PRO^{404},PHE^{487},ILE^{491},GLY^{621},TYR^{623},ASP^{625},GLU^{626},HIS^{627},PHE^{628}, ARG^{634}, ARG^{635}, ILE^{637},ALA^{638}
Site 10	202	GLN^{108},TRP^{109},LEU^{110},GLU^{111},GLY^{112},ALA^{113},GLY^{114},THR^{115},LEU^{116},MET^{148}, GLU^{171}, LEU^{172}, ASN^{173}